

# LRWD1 Regulates Microtubule Nucleation and Proper Cell Cycle Progression in the Human Testicular Embryonic Carcinoma Cells

Chia-Yih Wang,<sup>1,2</sup> Yu-Han Hong,<sup>3</sup> Jhih-Siang Syu,<sup>1,2</sup> Yung-Chieh Tsai,<sup>4,5,6</sup> Xiu-Ying Liu,<sup>3</sup> Ting-Yu Chen,<sup>1,2</sup> Yin-Mei Su,<sup>3</sup> Pao-Lin Kuo,<sup>7</sup> Yung-Ming Lin,<sup>8</sup> and Yen-Ni Teng<sup>3\*</sup>

<sup>1</sup>Department of Cell Biology and Anatomy, College of Medicine, National Cheng Kung University, Tainan 701, Taiwan

<sup>2</sup>Institute of Basic Medical Sciences, College of Medicine, National Cheng Kung University, Tainan 701, Taiwan

<sup>3</sup>Department of Biological Sciences and Technology, National University of Tainan, Tainan 700, Taiwan

<sup>4</sup>Department of Obstetrics and Gynecology, Chi-Mei Medical Center, Tainan, Taiwan

<sup>5</sup>Department of Medicine, Taipei Medical University, Taipei, Taiwan

<sup>6</sup>Department of Sport Management, Chia Nan University of Pharmacy and Science, Tainan, Taiwan

<sup>7</sup>Department of Obstetrics and Gynecology, College of Medicine, National Cheng Kung University, Tainan 701, Taiwan

<sup>8</sup>Department of Urology, College of Medicine, National Cheng Kung University, Tainan 701, Taiwan

## ABSTRACT

Leucine-rich repeats and WD repeat domain containing protein 1 (LRWD1) is a testis-specific protein that mainly expressed in the sperm neck where centrosome is located. By using microarray analysis, LRWD1 is identified as a putative gene that involved in spermatogenesis. However, its role in human male germ cell development has not been extensively studied. When checking in the semen of patients with asthenozoospermia, teratozoospermia, and asthenoteratozoospermia, the level of LRWD1 in the sperm neck was significantly reduced with a defective neck or tail. When checking the sub-cellular localization of LRWD1 in the cells, we found that LRWD1 resided in the centrosome and its centrosomal residency was independent of microtubule transportation in NT2/D1, the human testicular embryonic carcinoma, cell line. Depletion of LRWD1 did not induce centrosome re-duplication but inhibited microtubule nucleation. In addition, the G1 arrest were observed in LRWD1 deficient NT2/D1 cells. Upon LRWD1 depletion, the levels of cyclin E, A, and phosphorylated CDK2, were reduced. Overexpression of LRWD1 promoted cell proliferation in NT2/D1, HeLa, and 239T cell lines. In addition, we also observed that autophagy was activated in LRWD1 deficient cells and inhibition of autophagy by chloroquine or bafilomycin A1 promoted cell death when LRWD1 was depleted. Thus, we found a novel function of LRWD1 in controlling microtubule nucleation and cell cycle progression in the human testicular embryonic carcinoma cells. *J. Cell. Biochem.* 119: 314–326, 2018. © 2017 Wiley Periodicals, Inc.

**KEY WORDS:** LRWD1; CENTROSOME; CELL CYCLE; MICROTUBULE NUCLEATION; AUTOPHAGY

**L**eucine-rich repeats and WD repeat domain containing protein 1 (LRWD1, also known as ORC-associated protein, ORCA) is identified as a novel candidate involved in human spermatogenesis

obtained from cDNA microarray analysis of patients with severe spermatogenic defects [Lin et al., 2006]. In the somatic cells, LRWD1 functions as a scaffold for the establishment of histone H3 lysine 9

Conflicts of interest: The authors declare no conflict of interest.

Grant sponsor: National Science Council of Taiwan; Grant numbers: NSC 102-2314-B-024-001, 101-2311-B-024-001, NSC 99-2314-B-024-001-MY3; Grant sponsor: Ministry of Science and Technology of Taiwan; Grant numbers: MOST 103-2314-B-024-002, MOST 104-2314-B-024-002-MY2.

\*Correspondence to: Prof. Yen-Ni Teng, Ph.D, Department of Biological Sciences and Technology, National University of Tainan, No.33, Sec. 2, Shulin St West Central District, Tainan 700, Taiwan. E-mail: tengyenni@mail.nutn.edu.tw; tengyenni1968@gmail.com

Manuscript Received: 24 February 2017; Manuscript Accepted: 31 May 2017

Accepted manuscript online in Wiley Online Library (wileyonlinelibrary.com): 1 June 2017

DOI 10.1002/jcb.26180 • © 2017 Wiley Periodicals, Inc.

methylation via lysine methyltransferases complex for the organization of heterochromatin structure [Giri et al., 2015]. In the germ cells, LRWD1 is mainly expressed in the cytoplasm during spermiogenesis and it localizes to the neck region, where centrosome can be detected, of the mature sperm [Teng et al., 2010], suggesting that LRWD1 might be a centrosomal protein.

Centrosome, which consists of a pair of centrioles surrounded by the amorphous pericentriolar material, is the major microtubule nucleating site during interphase and orchestrates mitotic spindle at M phase in the mammalian cells [Doxsey, 2001]. By docking on the centrosome,  $\gamma$ -tubulin ring complex nucleates microtubule from minus end to the plus end for orchestrating microtubule networks [Hinchcliffe and Sluder, 2001]. Besides, centrosome is also a cell cycle coordinating center [Lambrus et al., 2016; Meitinger et al., 2016]. Depletion of centrosomal proteins, such as p150<sup>glued</sup>, leads to G1arrest [Chen et al., 2015a], and displacement of cyclin E and cyclin A from the centrosome inhibits S phase entry [Ferguson and Maller, 2010]. Proper functioning of CDK2, cyclin A, and E are required for G1/S transition [Pagano et al., 1992], however, centrosome also plays an important role in cell cycle progression.

Autophagy is a lysosomal-degradation process whereby cells maintain metabolic homeostasis [Hoyer-Hansen and Jaattela, 2008]. The autophagic flux can be activated by several cellular stresses, such as starvation, DNA damage, or hypoxia. In the nutrient-enrich environment, the Unc-51-like kinase 1 (ULK1) and -2 (ULK2) are inhibited by mammalian target of rapamycin (mTOR). Upon serum starvation, mTOR is inactivated thus ULK1/2 phosphorylates mammalian Atg13, focal adhesion kinase family interacting protein of 200 kDa (FIP200) to initiate autophagy [Jung et al., 2009]. Then, two ubiquitination-like processes are turned on for the autophagosome formation [Mizushima et al., 1998]. Atg12, the ubiquitin-like Atg protein, is activated by Atg7, an E1-like enzyme, and Atg10 then conjugated to Atg5 and promotes the formation of the autophagosome precursor. The other ubiquitin-like protein is microtubule-associated protein 1 light chain 3 (LC3). The LC3-I is transferred to Atg3, the E2-like enzyme, through a thioester bond, followed by conjugating to phosphatidylethanolamine (PE) to form the LC3-II. LC3-II associates with and promotes the formation of autophagosomes [Kabeya et al., 2000]. Once the autophagosome is formed, the following lysosomal fusion is required for the degradation of the autophagosomal content.

In this paper we found that LRWD1 localized to the centrosome. In the semen of patients with asthenozoospermia, teratozoospermia, and asthenoteratozoospermia, the level of LRWD1 was significantly reduced in the sperm neck. Depletion of LRWD1 led to poor microtubule nucleation in NT2/D1 cell line. In addition, we also found LRWD1 was required for proper cell growth. Overexpression of LRWD1 promoted cell growth, however, depletion of LRWD1 inhibited S phase entry by downregulating cyclin A and E. Furthermore, autophagy was activated in LRWD1 deficient cells for cell survival. Thus, we uncovered a novel function of LRWD1 in controlling microtubule nucleation and cell cycle progression for proper human testicular embryonic carcinoma cell growth.

## MATERIALS AND METHODS

### CELL CULTURE AND DRUG TREATMENT

NTERA-2 cl.D1N(NT2/D1), the human testicular embryonic carcinoma cell line, HeLa, human cervical cancer cell line, and 293T, human embryonic kidney cell line transformed with large T antigen, cell lines were grown in Dulbecco's modified Eagle medium (DMEM) medium supplemented with 10% fetal bovine serum at 37°C in a humidified atmosphere at 5% CO<sub>2</sub>. These cells were examined for the free of mycoplasma contamination by immunofluorescence regularly, and DAPI staining according to the guidelines. For drug treatment, cells were incubated with or without 10, 50, or 100  $\mu$ M chloroquine (Sigma, St. Louis, MO); or 1, 5, or 10 nM bafilomycin A1 (Enzo Life Sciences, Farmingdale, NY, USA) for 24 h before analysis.

### RNAi AND PLASMID TRANSFECTION

A lentiviral system for *LRWD1* gene silencing was obtained from the National RNAi Core Facility (Institute of Molecular Biology, Academia Sinica, Taipei, Taiwan). Short hairpin RNA (shRNA)-encoding pLKO.1 vectors were as follows:

pLKO.1-shluc (target sequence: 5'-CCTAAGGTTAAGTCGCCCTCG-3')

pLKO.1-sh322 (target sequence: 5'-CTCCTATGACAAGCGGATCAT-3')

pLKO.1-sh805 (target sequence: 5'-CAAGGATGCGTCCTCAAC TTA-3')

Lentiviruses were produced by cotransfection with *pLKO.1*, *pCMVdelIR8.91* and *pMD.G* for shRNA production in 293FT cells (Invitrogen, Carlsbad, CA) according to the protocols provided by the Taiwan National RNAi Core Facility.

The pcDNA3-Cyclin A-Venus-Flag and pcDNA3-HA-cyclin E were purchased from Addgene. For plasmid transfection, 6  $\mu$ l of Lipofectamine 2000 (Invitrogen) was mixed first with 500  $\mu$ l Opti-MEM medium (Life Technologies, Grand Island, NY) for 5 min, then with 2  $\mu$ g plasmid in 500  $\mu$ l Opti-MEM medium and incubated at room temperature for 20 min before the mixture was layered onto cells in 1 ml DMEM medium. Cells were harvested 24 or 48 h after transfection.

### HUMAN SUBJECTS AND SEMEN SAMPLE COLLECTION

The semen sample collection was approved by the Institutional Review Board of the Chi-Mei Medical Center of Taiwan (IRB approval numbers: Chi-Mei Medical Center of Taiwan IRB09808-006) and performed according to the protocol recommended by the World Health Organization using a modified Neubauer chamber WHO criteria [Cooper et al., 2010]. Semen samples were obtained from volunteers (25–35 years of age) after a minimum of 2 days and a maximum of 7 days of sexual abstinence. The diagnosis of all subjects was based on at least two separate semen samples analysis and two separate centrifuged semen samples analysis (3,000 *g* for 15 min). The patients included 44 with asthenozoospermia (motility lower than 50%, Astheno), 13 with teratozoospermia (more than 70% of pathological spermatozoa, Terato), and 12 with asthenoteratozoospermia (motility lower than 50%, more than 70% of pathological spermatozoa, A-T). Thirty-six fertile men with normal

semen parameters (motility higher than 50%, less than 70% of pathological spermatozoa, Normo) were recruited as a control group.

#### REVERSE TRANSCRIPTION-QUANTITATIVE POLYMERASE CHAIN REACTION (RT-qPCR)

Total RNA was extracted using Trizol reagent (Invitrogen) and subjected to reverse transcription using a High Capacity cDNA reverse transcription kit (Applied Biosystems). The resulting cDNAs were subjected to quantitative real-time PCR. PCR primers for the human LRWD1 and glyceraldehyde 3-phosphate dehydrogenase (GAPDH) genes were designed using the Primer Express software v2.0 (Applied Biosystems, Foster City, CA).

Human LRWD1 forward 5'-GGGGATTGTGCTCTGTGG-3' and reverse 5'-GGGGCCACTTCAGGATCT-3'.

GAPDH forward 5'-GAGTCCACTGGCGTCTTCAC-3' and reverse 5'-TTCACACCCATGACGAACAT-3'.

The RT-qPCR reactions were performed in a StepOnePlus™ Real-Time PCR Systems (Applied Biosystems) and a master mix containing Taq DNA polymerase in Power SYBR Green PCR Master Mix (Applied Biosystems). Each PCR reaction (20  $\mu$ l) contained 200 ng of cDNA template, 100 pmol each of the primer and its antisense oligonucleotide and 10  $\mu$ l of 2XSYBR Green I mixer. The reactions started with denaturation at 95°C for 10 min, followed by 40 cycles consisting of denaturation at 95°C for 15 s and annealing at 60°C for 60 s then the analysis by StepOne Software v2.1. All real-time experiments were performed in triplicates, and the mean mRNA values were calculated. Negative controls, without adding a template, were included in each set of RT-qPCR assays. The steady-state concentrations of LRWD1 mRNA in each testicular sample were normalized to the amount of GAPDH mRNA.

#### WESTERN BLOTTING ANALYSES

The following antibodies were obtained commercially: anti- $\gamma$ -tubulin (T6557), anti-cyclin A (C4710), and anti- $\alpha$ -tubulin (T9026), (Sigma), anti-CDK2 (#2546), anti-CDK2 phospho-Thr160 (#2561), anti-Cleaved Caspase-3 (Asp175) (#9661), and anti-LC3A/B (#12741) (Cell Signaling, Beverly, MA), anti-H2AX phospho-Ser139 (ab2893, Abcam, Cambridge, UK), anti-Beclin 1/ATG6 (NB500-249) (Novus, Littleton, CO), anti-cyclin E1 (HE-12, GTX23927), anti-actin (GTX109639), and anti-GAPDH (GTX100118) (Genetex, Irvine, CA), and anti-LRWD1 (AP11807a) (Abgent, San Diego, CA).

#### MTT ASSAY

Following lentivirus infection, cells were washed with PBS followed by adding 1 ml MTT solution (2 mg/ml in PBS) in each well. After incubation for 3 h at 37°C, 2 ml DMSO was added and incubation in the dark for additional 30 min. Absorbance was measured at the wavelength of 570 nm.

#### CELL CYCLE ANALYSIS

The cell cycle profile was analyzed by fluorescence-activated cell sorting (FACS) according to published method [Chen et al., 2015b]. Briefly, cells were collected by trypsinization and re-suspended with PBS. Following centrifugation at 1,000 rpm for 5 min, cells were re-suspended with PBS-E (1 mM EDTA in PBS). After centrifugation, the

pellet was re-suspended with 0.5 ml PBS-E and fixed with ice-cold 70% ethanol overnight at 4°C. Fixed cells were washed with PBS-E and stained with propidium iodide (PI, SouthernBiotech, Birmingham, AL) at room temperature for 1 h. DNA content of PI stained cells was measured by FACScan (Becton-Dickinson, San Diego, CA) and further analyzed by Kaluza software (Beckman Coulter, Brea, CA).

#### MICROTUBULE NUCLEATION ASSAY

Microtubule was depolymerized by treating cells with 25  $\mu$ M nocodazole in the culture medium for 1 h. For chasing repolymerization of the microtubule networks, the depolymerized cells were washed with PBS then culture in 37°C fresh medium for 5 min. At the indicated time point in each experiment, the cells were fixed by ice-cold methanol followed by immunofluorescence staining with antibodies against  $\alpha$ - and  $\gamma$ -tubulins.

#### EdU INCORPORATION ASSAY

For EdU incorporation assay, EdU positive cells were stained by detecting fluorescence EdU signaling according to manufacturer's instruction (Invitrogen). Cells were co-stained with DAPI to visualize nuclei. EdU incorporation assay was performed in asynchronized cells after LRWD1 depletion for 3 days; or after LRWD1 was depleted for three days with 24 h starvation for cell synchronization in G0/G1 phase. Following synchronization, serum and EdU were added to the culture medium for different time period (0.5, 1, and 2 h).

#### STATISTICAL ANALYSIS

All results are expressed as the mean  $\pm$  S.D. from at least three independent experiments, more than 100 cells were counted in each individual group. Differences between two groups were compared using unpaired two-tailed *t*-tests, for which a *P*-value < 0.05 was considered to be statistically significant.

## RESULTS

#### LRWD1 mRNA LEVELS IN PATIENTS WITH DIFFERENT TESTICULAR HISTOPATHOLOGY

To elucidate the possible function of human LRWD1 in male germlines, the localization of LRWD1 in ejaculated sperm was also investigated. In normal human sperm, LRWD1 was detected in the sperm neck and was colocalized with centrin, the centrosomal marker (Fig. 1A). Since the sperm neck is important for sperm tail formation and orchestrates the microtubule scaffold of sperm flagella, we hypothesized that LRWD1 played an important role in the normal sperm formation. We further compared the expression of LRWD1 in the ejaculated sperm from normal controls and patients with morphologically defective sperm. The human subjects included 44 with asthenozoospermia (Astheno), 13 with teratozoospermia (Terato), 12 with asthenoteratozoospermia (A-T), as well as 36 with normal semen parameters (Normal). We first determined the levels of LRWD1 mRNA in the sperm by RT-qPCR. The levels of LRWD1 mRNA in patients with sperm defects were significantly lower than those of the normal controls (Fig. 1B). The LRWD1 mRNA levels were significantly decreased in Astheno (*P* < 0.0001, *n* = 44), Terato (*P* = 0.0017, *n* = 13), and A-T (*P* = 0.0048, *n* = 12) compared with

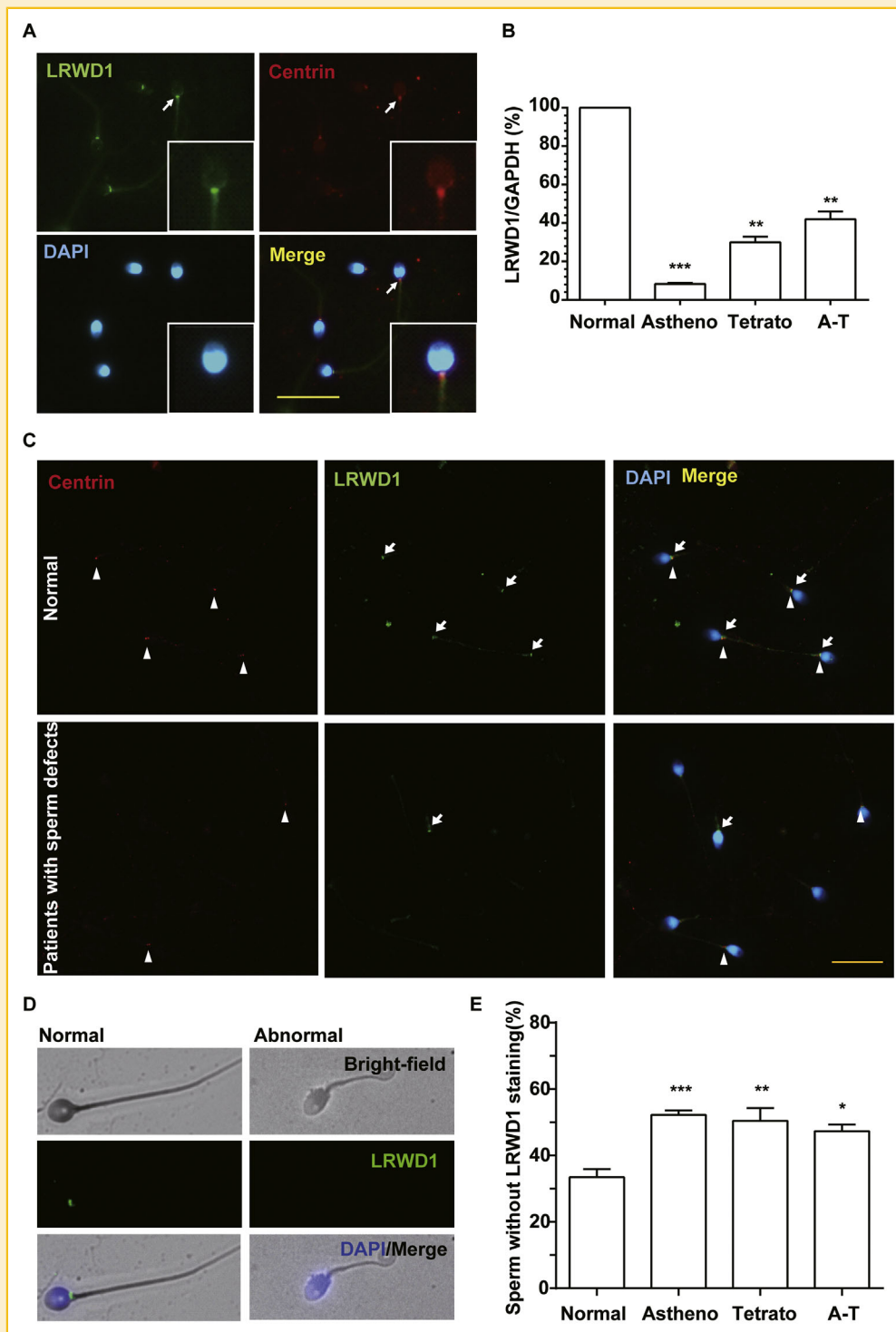


**Fig. 1.** The expression pattern of LRWD1 in the human sperm. (A) LRWD1 signal was concentrated at the sperm neck and colocalized with centrin. LRWD1: green, centrin: red, nuclei stained with DAPI: blue. (B) Analysis of LRWD1 mRNA levels in the semen samples of normal subjects and patients with sperm defects. LRWD1 mRNA levels in normal semen controls (Normal,  $n = 36$ ) and patients with asthenozoospermia (Asthenzo,  $n = 44$ ), teratozoospermia (Terato,  $n = 13$ ) and asthenoteratozoospermia (A-T,  $n = 12$ ) were determined by RT-qPCR and normalized to the levels of GAPDH mRNA. Data represent the mean  $\pm$  SD.  $**P < 0.01$ ,  $***P < 0.001$ , calculated by the unpaired student's  $t$ -test. (C-E) Reduced LRWD1 signal in the sperm neck of patients with sperm defects. (C-D) Immunofluorescence staining showed less LRWD1 and centrin signals located in morphological defect sperm. LRWD1: green, as indicated by the arrow; centrin: red, as indicated by the arrow head; nuclei stained with DAPI: blue. Scale bars are 10  $\mu$ m. (E) Quantitation result of (C) in normal semen controls and patients with asthenozoospermia, teratozoospermia, and asthenoteratozoospermia. Data represent the mean  $\pm$  SD.  $*P < 0.05$ ,  $**P < 0.01$ ,  $***P < 0.001$ , calculated by the unpaired student's  $t$ -test.

Normal ( $n = 36$ ). We next compared the population of sperm lacking LRWD1 signal in patient and the control groups. In general, the population of sperm with less LRWD1 signal was significantly increased in the semen samples of patients with asthenozoospermia, teratozoospermia, and asthenoteratozoospermia compared with from that of the normal subjects (Fig. 1C–E). In addition, we also observed the population of sperm with less centrin signal was increased in patients with sperm defects, suggesting a potential neck defects in patient's spermatozoa (Fig. 1C). These result thus indicated an association between decreased LRWD1 expression and structure-defects in human sperm.

#### LRWD1 RESIDES IN THE CENTROSOME IN CELL CYCLE DEPENDENT MANNER

LRWD1 located in the sperm neck and colocalized with centrin, suggesting that LRWD1 might be a centrosomal protein. To further confirm this, double staining of LRWD1 with  $\gamma$ -tubulin, the centrosomal marker, was performed in pluripotent human testicular embryonic carcinoma NT2/D1 cell line. As expected, LRWD1 was colocalized with  $\gamma$ -tubulin (Fig. 2A). To rule out the signal of LRWD1 in the centrosome was due to the non-specific interaction of

antibody, the LRWD1 was depleted by shRNA. LRWD1 was depleted by shRNA against LRWD1 (sh805) efficiently (Fig. 2B); consistently, the centrosomal signal of LRWD1 was also reduced (Fig. 2C), supporting the LRWD1 located in the centrosome. Microtubule arrays might affect the targeting of centrosomal proteins, we then checked whether centrosomal localization of LRWD1 depended on the microtubule transport. Without microtubule depolymerization, LRWD1 was detected in the centrosome (Fig. 2D). When microtubule was depolymerized, however, LRWD1 was still localized in the centrosome as shown by co-localized with  $\gamma$ -tubulin, suggesting the centrosomal targeting of LRWD1 was independent of microtubule transport.

Centrosomal proteins show dynamic distribution during different cell cycle stages [Chen et al., 2015a], the centrosomal targeting of LRWD1 was further examined in different cell cycle stages. During interphase (G1 phase, one  $\gamma$ -tubulin spot; S phase, two duplicated adjacent  $\gamma$ -tubulin spots; G2 phase, the duplicated centrosomes start to separate apart from each other), LRWD1 resided in the centrosome (Fig. 3A). Entering into mitosis, LRWD1 was still present in the centrosomes (mitotic spindle poles) throughout the mitosis, and the LRWD1 signal was also detected in the midbody during cytokinesis

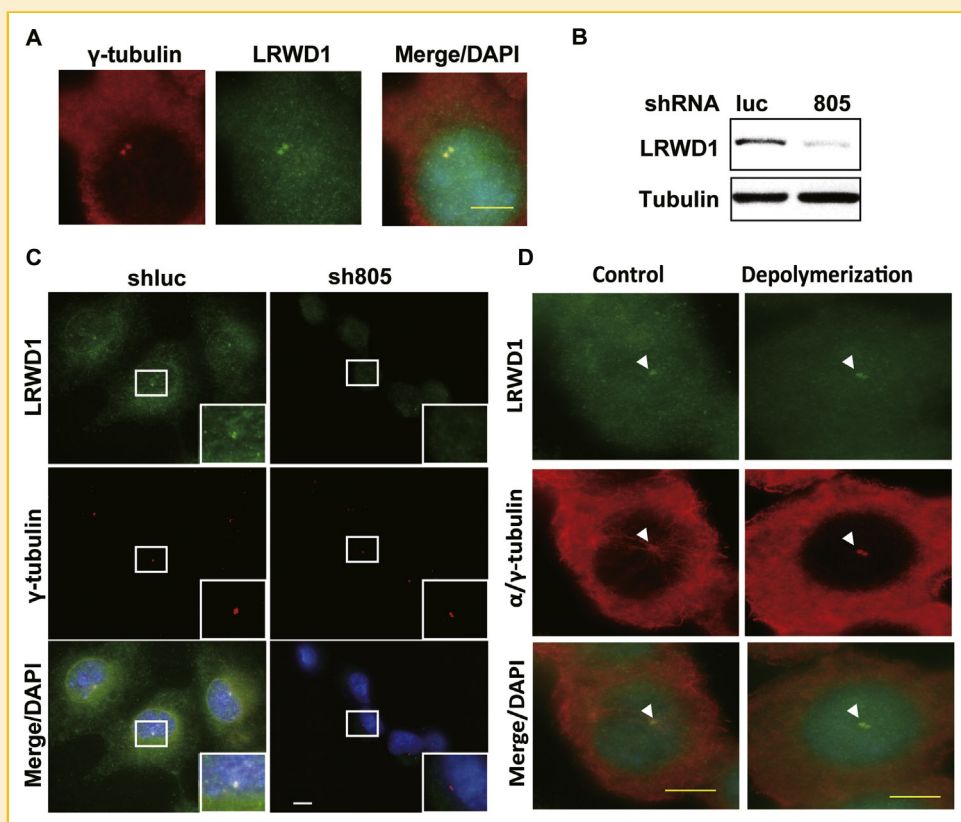


**Fig. 2.** The centrosomal localization of LRWD1 in NT2/D1 cells. (A–C) LRWD1 localized in the centrosome. (A) LRWD1 colocalized with  $\gamma$ -tubulin as shown by Immunofluorescence staining with antibodies against LRWD1 and  $\gamma$ -tubulin. (B) LRWD1 was depleted efficiently by infected with lentivirus containing shRNA against LRWD1 (sh805). Extracts of LRWD1 depleted cells (sh805) and control cells (shluc) were analyzed by Western blotting assay with antibodies against LRWD1 and tubulin. (C) Centrosomal LRWD1 signal was reduced in LRWD1 deficient cells as shown by Immunofluorescence staining with antibodies against LRWD1 and  $\gamma$ -tubulin. (D) Centrosomal localization of LRWD1 was microtubule independently. Centrosomal targeting of LRWD1 was checked by Immunofluorescence staining of normal (control) or microtubule-depolymerized cells with antibodies against LRWD1 (green) and microtubule plus with centrosome,  $\alpha$ -tubulin, and  $\gamma$ -tubulin ( $\alpha/\gamma$ -tubulin, red), respectively. DNA was stained with DAPI.

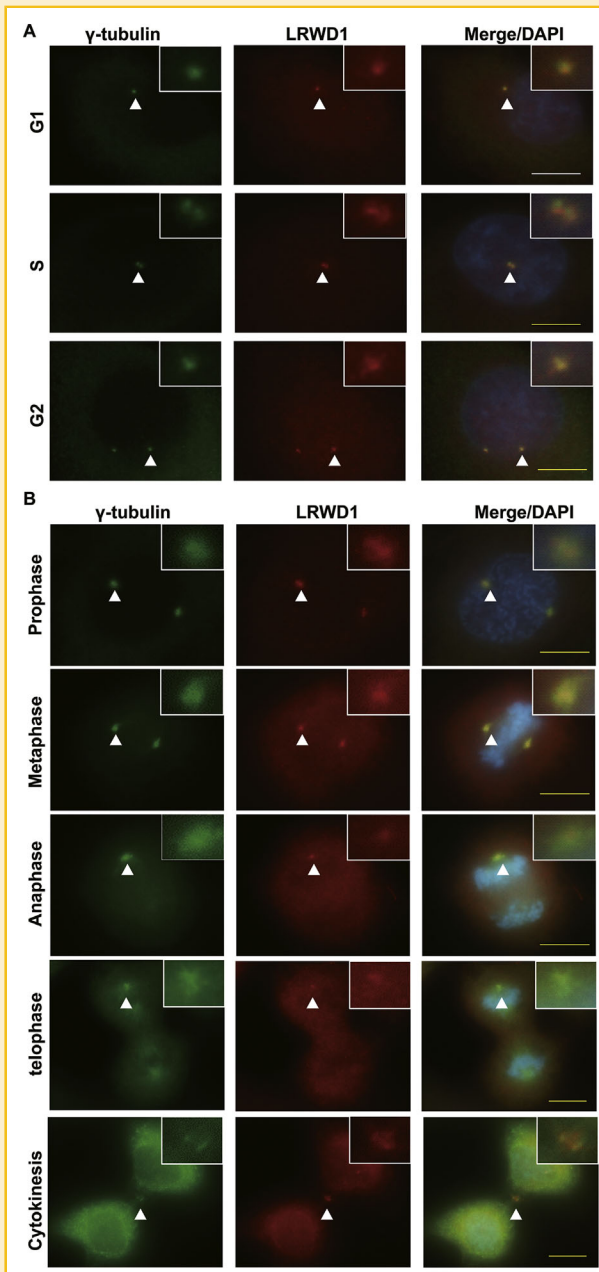


Fig. 3. The expression pattern of LRWD1 in different cell cycle stages in NT2/D1 cells. (A and B) The expression pattern of LRWD1 was examined by immunofluorescence staining of NT2/D1 cells during interphase (A) or M phase (B) with antibodies against LRWD1 (green) and  $\gamma$ -tubulin (red). The nuclei stained with DAPI: blue. Scale bars are 10  $\mu$ m. The arrow head indicates the centrosome (interphase), mitotic spindle poles (mitosis), and midbody (cytokinesis).

(Fig. 3B). Thus, centrosomal targeting of LRWD1 was independent of cell cycle stages.

#### LRWD1 MAINTAINS MICROTUBULE NUCLEATION

The role of LRWD1 in the centrosome was further examined. Depletion of centrosomal proteins, such as NR5A1 and Cep76, leads

to centrosome amplification (cells with more than two centrosomes) [Tsang et al., 2009; Lai et al., 2011]. LRWD1 was a centrosomal protein, the centrosome copy numbers then were checked in LRWD1 deficient cells. After depletion of LRWD1 by shRNA for 3 days, centrosome amplification was not observed in LRWD1 deficient cells (Supplementary Fig. S1A and B). We then checked whether depletion of LRWD1 suppressed centrosome amplification. As the basal population of cells with multiple centrosomes was low in LRWD1 cell line, NT2/D1 cells were treated with hydroxyurea, an anti-cancer drug induces centrosome re-duplication efficiently [Wang et al., 2015], when LRWD1 was depleted. Hydroxyurea induced centrosome re-duplication in NT2/D1 cells, however, depletion of LRWD1 even did not suppress or promote this phenotype (Fig. S1A and B). These data suggested that LRWD1 did not regulate centrosome re-duplication.

Centrosome is the microtubule nucleating site, we further investigated whether LRWD1 was required for the architecture of the microtubule. LRWD1 depletion by sh805 caused microtubule lost its filamentous structure and diffused throughout the cytoplasm, peripheral extensions of the cells to shrink, and cell shape was not maintenance (Fig. 4A and B), suggesting LRWD1 might participate in the microtubule nucleation. To further confirm LRWD1 functioned in the microtubule nucleation, microtubule regrowth assay was performed. Microtubule was depolymerized by treating with nocodazole followed by culturing in 37°C fresh medium for 5 min for chasing repolymerization of the microtubule networks. Nocodazole disrupted microtubule networks efficiently (Fig. 4C, left panel). After the drug was washed away, the  $\alpha$ -tubulin threads extended from the base of  $\gamma$ -tubulin in control cells, suggesting microtubules were re-polymerized (Fig. 4C, right panel). However, the ability of microtubule to regrow was reduced dramatically when LRWD1 was depleted, indicating depletion of LRWD1 reduced the microtubule nucleation ability of NT2/D1 cells.

#### LRWD1 IS REQUIRED FOR PROPER CELL CYCLE PROGRESSION

In addition to nucleating microtubule networks, centrosome is also known as a cell cycle coordinating hub [Doxsey, 2001]. We then tested whether LRWD1 was participated in cell growth. Following LRWD1 depletion for 72 h, the cell numbers were reduced dramatically and this was further confirmed by MTT assay (Fig. 5A–D), suggesting LRWD1 was required for proper cell growth. Next, we examined cell-cycle profiles by flow cytometry after LRWD1 depletion for 72 h. Three days after LRWD1 depletion, the proportions of subG1 (apoptotic cells) in LRWD1 depleted cells was reminiscent of control cells indicating that depletion of LRWD1 did not induce apoptosis (Fig. 5E). To further this, cleaved-caspase 3, the marker of apoptosis, was examined by Western blotting assay. Etoposide, an anti-cancer drug that triggers apoptosis by increasing the level of cleaved-caspase 3 [Wang et al., 2013], was used as positive control. Cleaved-caspase 3 was increased in etoposide-treated cells, however, depletion of LRWD1 did not increase the abundance of cleaved-caspase 3 (Fig. 5F). In addition, no DNA damage responses were observed in LRWD1 deficient cells (Fig. 5G) as shown by  $\gamma$ H2AX staining, a marker of DNA damage responses [Wang et al., 2015]. These data indicated depletion of LRWD1 did not induce apoptosis or DNA damage responses in NT2/D1 cell lines.

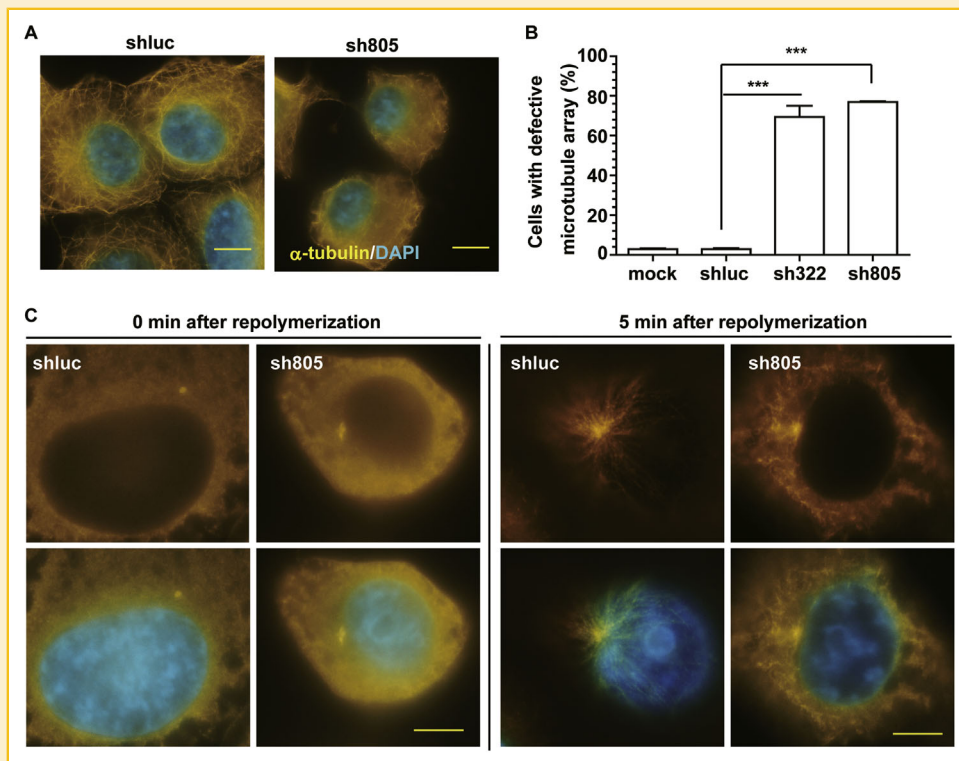


**Fig. 4.** LRWD1 regulates microtubule nucleation of the centrosome in NT2/D1 cells. (A and B) Disorganized microtubule networks were observed in LRWD1 deficient NT2/D1 cells. (A) Immunofluorescence staining of cells infected with lentivirus containing shRNA against control (shluc) or LRWD1 (sh805) with antibody against  $\alpha$ -tubulin. (B) Quantitation results of (A).  $***P < 0.001$ . (C) LRWD1 regulated microtubule nucleation in NT2/D1 cells. Microtubules were depolymerized by nocodazole (10  $\mu$ g/ml) treatment for 60 min (Left panel), followed by chase in 37°C fresh medium for 5 min to regrow the microtubule networks (right panel). The upper panel showed microtubule ( $\alpha$ -tubulin); the lower panel showed DAPI merge with microtubule.

As shown by flow cytometry analysis, the population of cells at G1 phase was increased whereas that at S phase was reduced (Fig. 5E). The ability of cells to enter into S phase was then studied by 5-ethynyl-2'-deoxyuridine (EdU) incorporation assay. Consistent with our flow cytometry analysis, depletion of LRWD1 reduced EdU incorporation in NT2/D1 cells (Fig. 6A and B). To further confirm this, NT2/D1 cells were infected with lentivirus containing shRNA against luciferase or LRWD1 for 3 days and these cells were starved at the last 24 h for synchronization in G0/G1 phase. Following synchronization, serum, and EdU were added to the culture medium for different time period (0.5, 1, and 2 h). As expected, depletion of LRWD1 by sh322 and sh805 reduced EdU incorporation in NT2/D1 cell line (Fig. 6C). Thus, LRWD1 was required for S phase entry. Proper microtubule organization is required for mitotic entry [Jackson et al., 2007], we therefore, examined whether LRWD1 depletion affected mitosis entry. As expected, depletion of LRWD1 blocked mitosis entry as shown by reduced mitotic index (Fig. 6D). Taken together, LRWD1 was required for proper cell growth by regulating G1/S transition.

Cell cycle progression is regulated by the activity of CDKs, which are activated or inactivated by the binding partners or the inhibitors, respectively [Morgan, 1995]. We further checked the expression of cell cycle-related regulators. Activation of p53 (phosphorylation of p53 at Ser15) is known to inhibit S phase entry [Mikule et al., 2007], we then checked the level of phosphorylated p53. The levels of phosphorylated or

total p53 were not affected by LRWD1 depletion (Fig. 6E). However, when analyzed the cell lysate of LRWD1 depleted NT2/D1 cells, the levels of cyclin A and E, critical cyclins for S phase entry, were reduced (Fig. 6F). In addition, the phosphorylated CDK2, but not the total CDK2, was also reduced. To further confirm the role of cyclin E and A in regulating cell growth, these cyclins were ectopically expressed in LRWD1 deficient cells. Depletion of LRWD1 inhibited cell growth, however, overexpression of cyclin E or A ameliorated reduced cell growth when LRWD1 was knocked down (Fig. 6G). Thus, reduced expression of cyclin A and E led to G1 arrest in LRWD1 deficient NT2/D1 cells.

Depletion of LRWD1 inhibited cell proliferation, we then tested whether overexpression of LRWD1 promoted cell growth. FLAG-tagged LRWD1 was overexpressed in NT2/D1, 293T, and HeLa cell lines, and we found the cell numbers were increased in those LRWD1-overexpressed cell lines (Fig. 7A–C). When checking the cell cycle related cyclins, as expected, the levels of cyclin A, E, and phosphorylated CDK2 were increased in LRWD1-overexpressed cells (Fig. 7D and E). Thus, the level of LRWD1 was required for proper cell growth.

#### AUTOPHAGY MAINTAINS CELL VIABILITY IN LRWD1 DEFICIENT CELLS

Autophagy is known as a protective mechanism for cell survival when cells suffer from stresses [Codogno and Meijer, 2005], we then

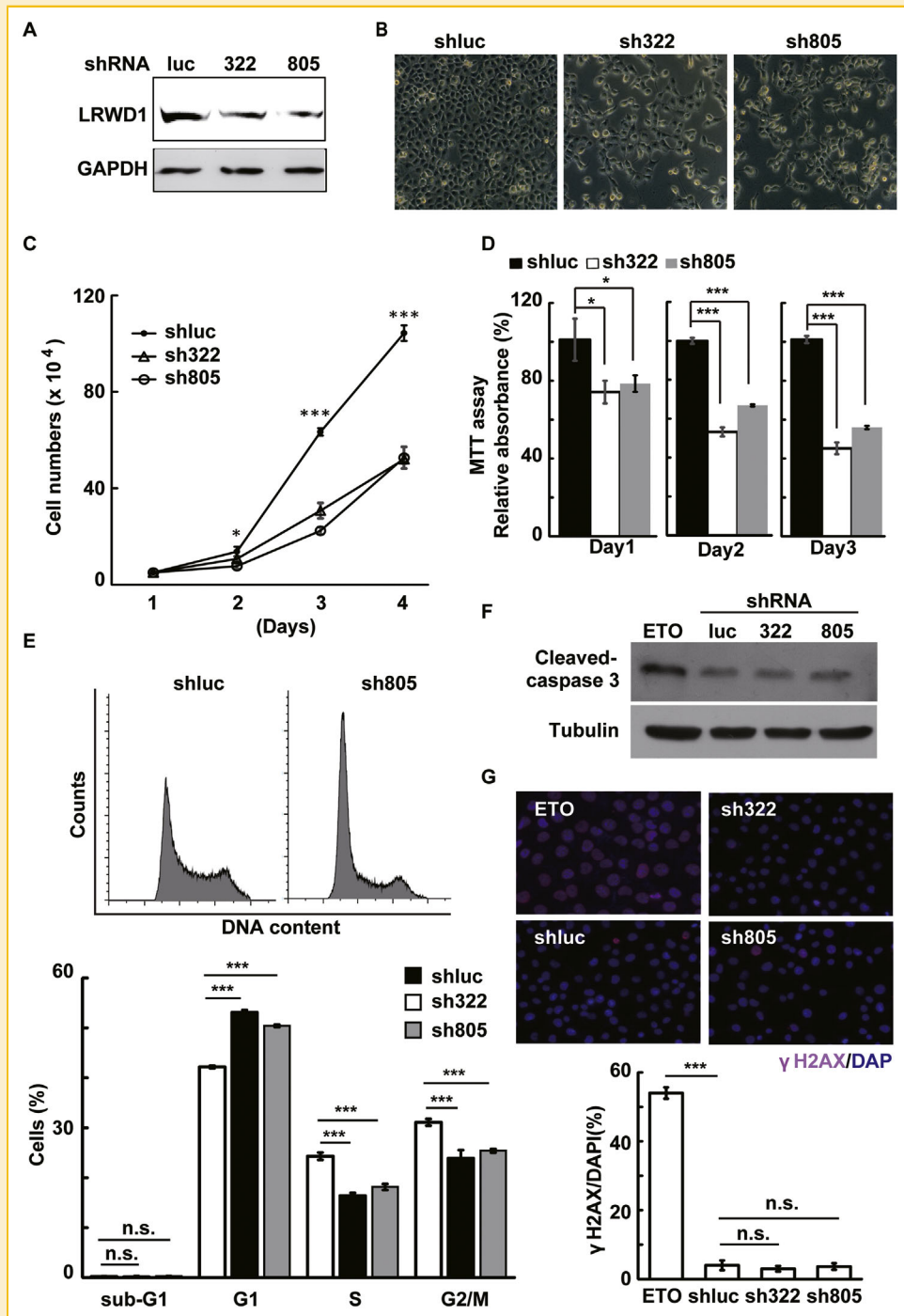
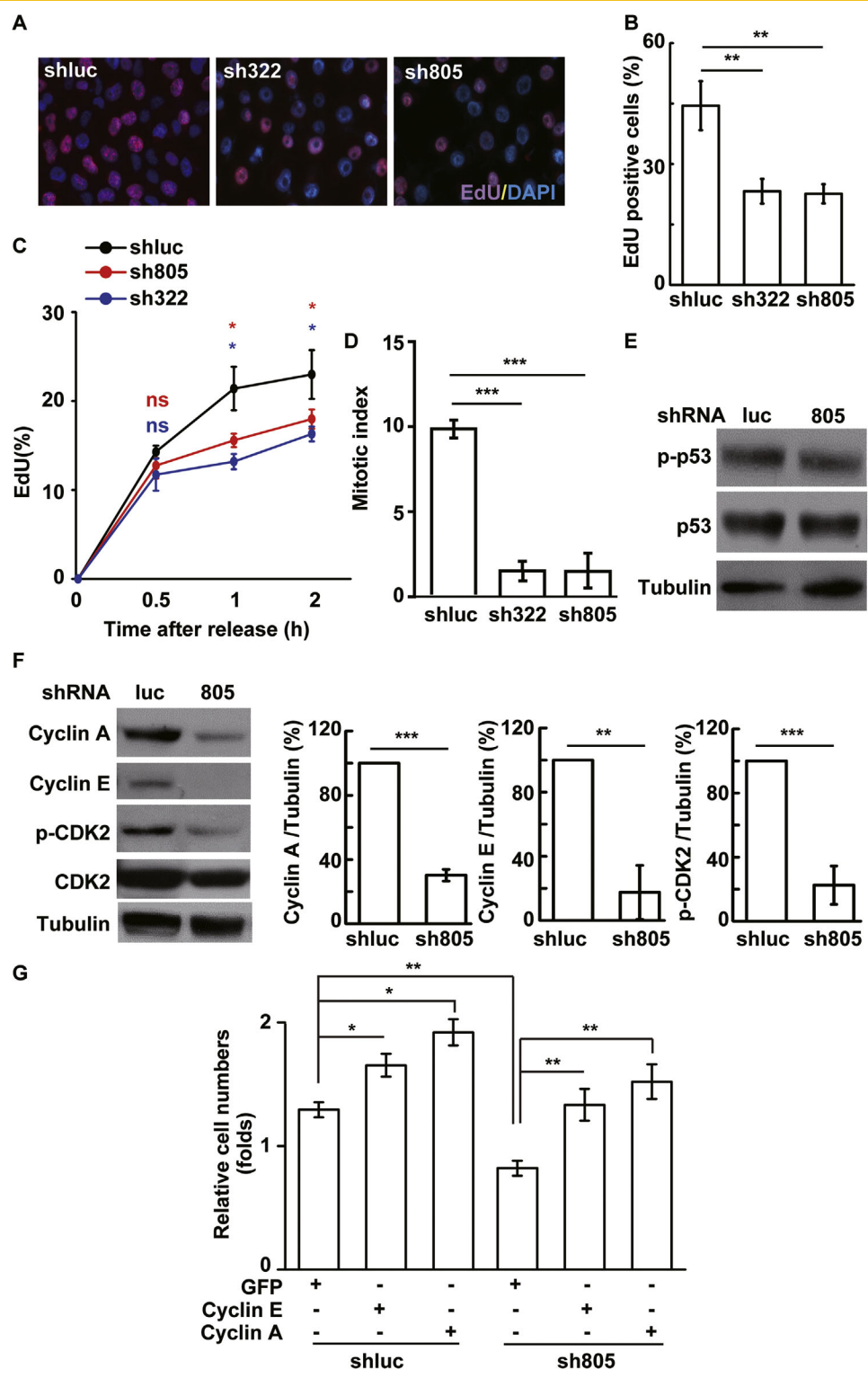


Fig. 5. Depletion of LRWD1 reduces NT2/D1 cell growth. (A) Depletion of LRWD1 by shRNA (sh322 or sh805) efficiently. (B–D) Depletion of LRWD1 reduced NT2/D1 cell growth. The cell numbers (B and C) and viable cells (D) were quantified in scramble control (shluc) or LRWD1 depleted cells in time dependent manner (C and D). (E) Depletion of LRWD1 did not induce apoptosis, but led to G1 arrest. Cell cycle profile analysis LRWD1 depleted NT2/D1 cells by flow cytometry analysis. (F) Cleaved-caspase 3 was not triggered by depletion of LRWD1. Extracts of shluc, sh322, and sh805 depleted cells or etoposide (ETO) treated cells (positive control) were analyzed by Western blotting assay with antibodies against cleaved-caspase 3 or tubulin. (G) Depletion of LRWD1 did not induce DNA damage response. DNA damage response was examined by immunofluorescence staining of cells with antibody against  $\gamma$ H2AX (upper part). The quantitation results of upper images (lower part) was shown in the lower panel. ETO treatment served as positive control. n.s., no significance;  $***P < 0.001$ .



**Fig. 6.** Depletion of LRWD1 reduces G1/S transition. (A–C) The ability of cells entered into S phase was reduced in LRWD1 depleted NT2/D1 cells. (A) Immunofluorescence staining of EdU (red) and DAPI (blue) in scramble control (shluc) or LRWD1 depleted (sh322 or sh805) NT2/D1 cells. Quantitation of EdU incorporation in asynchronous cells (B) or in cells which were starved for 24 h followed by chasing in full medium (C). These results are mean  $\pm$  SD from three independent experiments; more than 1000 cells were counted in each individual group. (D) Mitotic index was quantified in scramble control (shluc) or LRWD1 depleted (sh322 or sh805) NT2/D1 cells. (E) Depletion of LRWD1 did not activate p53. Extracts of LRWD1 depleted NT2/D1 cells were analyzed by Western blotting assay with antibodies against p53, phosphorylated p53 at Ser15 (p-p53), and tubulin. (F) Depletion of LRWD1 reduced the levels of cyclin A, E, and phosphorylated CDK2. Extracts of LRWD1 depleted NT2/D1 cells were analyzed by Western blotting assay with antibodies against cyclin A, cyclin E, phosphorylated CDK2 at Thr160 (p-CDK2), CDK2, and tubulin. Right panel: quantification results of (E). \*\* $P < 0.01$ ; \*\*\* $P < 0.001$ . (G) Overexpression of cyclin A or E rescued the growth defect in LRWD1 depleted cells. Quantitation results of cells overexpressed GFP, cyclin A, or cyclin E in control (shluc) or LRWD1 deficient (sh805) cells. \* $P < 0.05$ ; \*\* $P < 0.01$ .

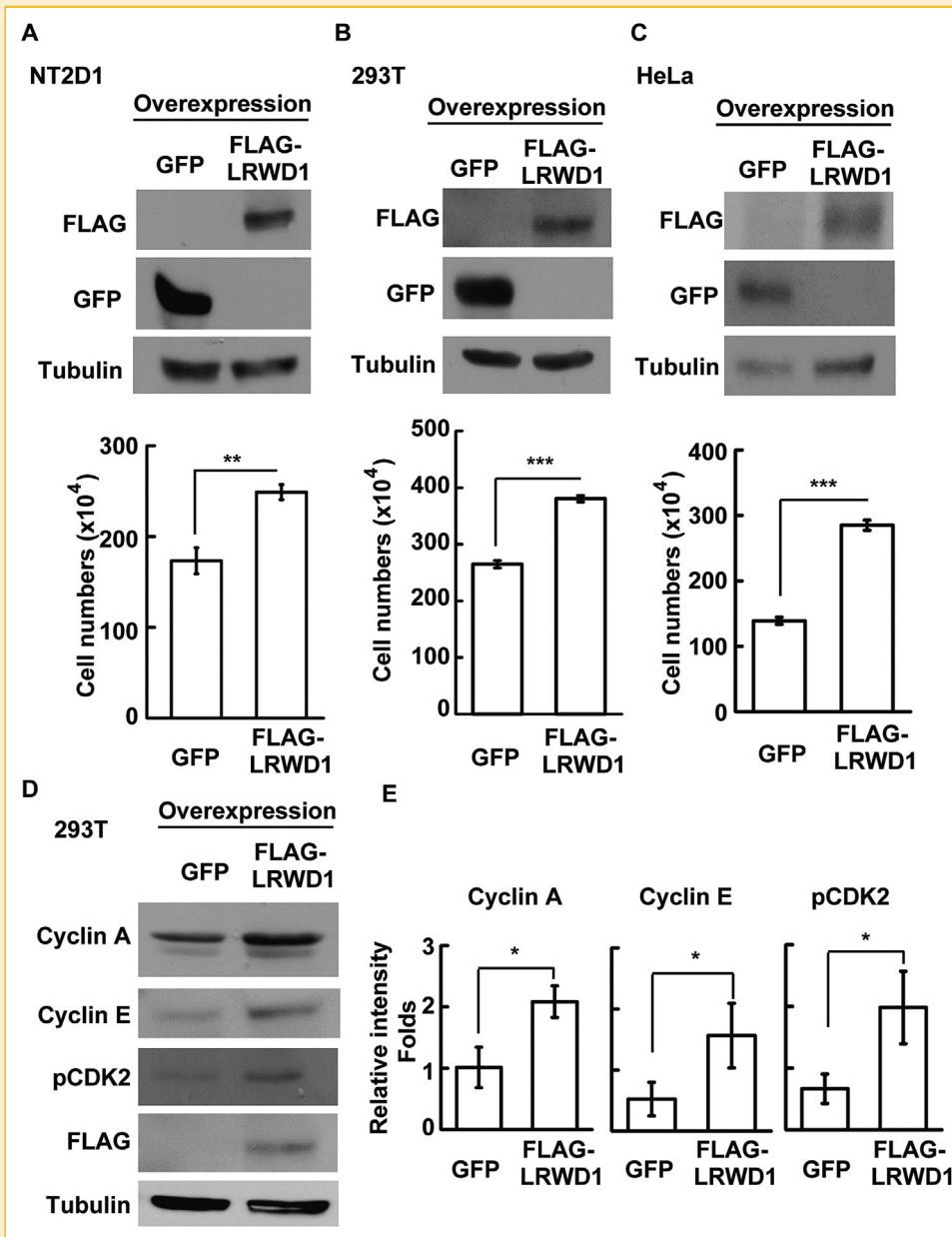
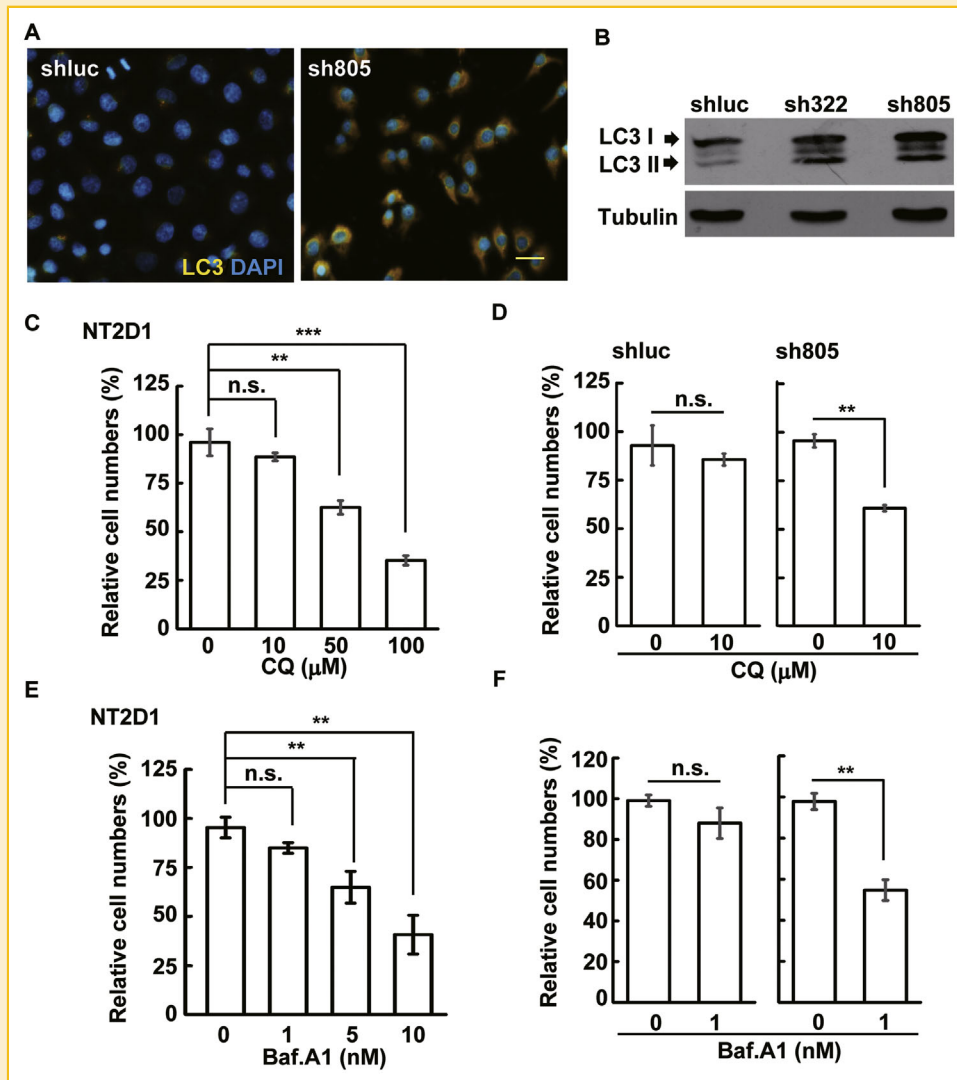


Fig. 7. Overexpression of LRWD1 promotes cell proliferation. (A–C) Overexpression of LRWD1 promoted cell growth in NT2/D1 (A), 293T (B), and HeLa (C) cell lines. Upper panel: extracts of GFP or FLAG-tagged LRWD1 cells were analyzed by Western blotting assay with antibodies against FLAG, GFP, and tubulin. Lower panel: quantitation results of the cell numbers of GFP- or LRWD1-overexpressed cells. (D–E) The levels of cyclin A, E, and phosphorylated CDK2 were increased in 293T cells. (D) Extracts of LRWD1-overexpressed 293T cells were analyzed by Western blotting assay with antibodies against cyclin A, cyclin E, phosphorylated CDK2 at Thr160 (p-CDK2), FLAG, and tubulin. (E) Quantification results of (D). \* $P < 0.05$ ; \*\* $P < 0.01$ ; \*\*\* $P < 0.001$ .

checked whether depletion of LRWD1 induced autophagy. In the control cells, LC3 puncta were hardly to be detected. However, LC3 puncta were accumulated in the cytoplasm in LRWD1 deficient cells (Fig. 8A). Accumulation of LC3 puncta might due to increased autophagy activity or the block of autophagic flux, thus, the conversion of LC3 I to II was examined. In the control cells, the level of LC3 II was low. When LRWD1 was depleted, the level of LC3 II and the LC3 II to I ration, however were increased, suggesting depletion of LRWD1 induced autophagy (Fig. 8B). We then tested whether the

activation of autophagy protected cells from cell death in LRWD1 deficient cells. Autophagy inhibitor, chloroquine (CQ), was treated to the NT2/D1 cells and we found CQ concentration at 10  $\mu\text{M}$  did not affect cell viability. Next, we treated cells with 10  $\mu\text{M}$  CQ in control or LRWD1 deficient cells. In the control cells, 10  $\mu\text{M}$  CQ treatment did not affect cell viability; however, less cell viability was observed in LRWD1 depleted NT2/D1 cells (Fig. 8C and D). This phenomenon was further confirmed by treating cells with other autophagy inhibitor, bafilomycin A1 (Baf. A1) at 1 nM concentration



**Fig. 8.** Autophagy maintains cell viability in LRWD1 deficient NT2/D1 cells. (A and B) Depletion of LRWD1 induced autophagy. (A) Immunofluorescence staining of control (shluc) or LRWD1 depleted (sh805) cells with antibody against LC3. (B) Extracts of LRWD1 depleted cells were analyzed by Western blotting assay with antibodies against LC3 and tubulin. (C–F) Inhibition of autophagy reduced cell viability in LRWD1 deficient cells. (C and E) Inhibition of autophagy by chloroquine (CQ) (C) or bafilomycin A1 (Baf. A1) (E) did not affect NT2/D1 cell viability at low concentration. (D and F) Inhibition of autophagy reduced cell viability in LRWD1 deficient cells. n.s., no significance; \*\* $P < 0.01$ ; \*\*\* $P < 0.001$ .

(Fig. 8E and F). Thus, depletion of LRWD1 induced autophagy for the maintenance of cell viability.

## DISCUSSION

Here, we demonstrated that LRWD1 was a centrosomal protein, its depletion led to poor microtubule nucleation and reduced cell growth. On the contrary, overexpression of LRWD1 promoted cell proliferation. We also observed that autophagy was activated for maintaining cell survival in LRWD1 deficient cells. Thus, LRWD1 is important for proper testicular progenitor cell growth.

The activity of CDKs drive cell cycle progression [Morgan, 1995]. The CDK is activated when cyclin associates with the kinase, while the activated CDK will be inhibited by CDK

inhibitors. When cells suffer from stresses, p53 dependent G1 arrest are activated for the maintenance of genomic integrity [Dulic et al., 1994]. In LRWD1 deficient cells, the level of cyclin A and E were decreased thus attenuated the activity of CDK2 led to G1 arrest. In addition, no p53 activation or DNA damage responses were observed. LRWD1 is known to maintain chromatin structure, but its depletion did not induce DNA damage response, suggesting LRWD1 regulated cell growth mainly via regulating the level of cyclins.

Microtubule dynamics and cell cycle progression are tightly controlled by centrosome. Depletion of centrosomal proteins results in cell cycle arrest by preventing S phase entry [Mikule et al., 2007]. In addition, coupling centrosome with mitotic entry is important to maintain the orientation of mitotic

spindle [Gruber et al., 2011]. By using single-molecule pull-down assays, it has been suggested that LRWD1 forms a complex with and stabilizes histone H3 lysine 9 lysine methyltransferases complexes (H3K9 KMT) [Giri et al., 2015]. Alternated chromatin architecture and impaired replication timing are observed in LRWD1 deficient cells, suggesting that LRWD1 is crucial for the organization of heterochromatin structure. Here we demonstrated that depletion of LRWD1 also inhibited S phase entry due to downregulating cyclin A and E. In addition, LRWD1 was a critical factor to maintain microtubule network for proper cell cycle progression. Thus, in addition to maintaining chromatin architecture, LRWD1 also played a role in controlling the levels of cyclin A and E and microtubule nucleation for cell growth.

Autophagy is a lysosomal degradation process whereby cells degrade and reuse the old organelles and proteins to maintain metabolic homeostasis [Codogno and Meijer, 2005]. While it is primarily a mechanism to maintain cell metabolism, several cellular stresses, such as starvation, DNA damage, or hypoxia, increases the activity of autophagy for cell survival. Here, we showed that autophagy was activated in LRWD1 deficient cells and inhibition of autophagy suppressed cell viability. When LRWD1 was depleted, CQ and Baf. A1 can promote apoptosis thus NT2/D1 cells were more susceptible to cell death in the absence of LRWD1. So far it is still unclear why depletion of LRWD1 induces autophagy. We have identified several binding domains of Nrf2, a transcription factor that regulates redox signaling [Rossler and Thiel, 2017], in the promoter region of LRWD1, suggesting that LRWD1 may also participate in the redox homeostasis (data not shown). Thus, when LRWD1 was depleted, increased free radical might activate autophagy to maintain cell survival; once the autophagy was blocked, the protective effect might be attenuated leading to cell death. This hypothesis still needs to be tested.

## ACKNOWLEDGMENTS

This study was supported by grants from the National Science Council of Taiwan (NSC 102-2314-B-024-001, 101-2311-B-024-001, NSC 99-2314-B-024-001-MY3) and the Ministry of Science and Technology of Taiwan (MOST 103-2314-B-024-002, MOST 104-2314-B-024-002-MY2). We are grateful for the support from the Core Research Laboratory, College of Medicine, National Cheng Kung University. RNAi reagents were obtained from the National Core Facility for Manipulation of Gene Function by RNAi, miRNA, miRNA sponges, and CRISPR/Genomic Research Center, Academia Sinica, supported by the National Core Facility Program for Biotechnology Grants of MOST (MOST 104-2319-B-001-001-).

## REFERENCES

Chen TY, Syu JS, Han TY, Cheng HL, Lu FL, Wang CY. 2015a. Cell cycle-dependent localization of dynactin subunit p150 glued at centrosome. *J Cell Biochem* 116:2049–2060.

Chen TY, Syu JS, Lin TC, Cheng HL, Lu FL, Wang CY. 2015b. Chloroquine alleviates etoposide-induced centrosome amplification by inhibiting CDK2 in adrenocortical tumor cells. *Oncogenesis* 4:e180.

Codogno P, Meijer AJ. 2005. Autophagy and signaling: Their role in cell survival and cell death. *Cell Death Differ* 12(Suppl2):1509–1518.

Cooper TG, Noonan E, von Eckardstein S, Auger J, Baker HW, Behre HM, Haugen TB, Kruger T, Wang C, Mbizvo MT, Vogelsohn KM. 2010. World Health Organization reference values for human semen characteristics. *Hum Reprod Update* 16:231–245.

Doxsey SJ. 2001. Centrosomes as command centres for cellular control. *Nat Cell Biol* 3:E105–E108.

Dulic V, Kaufmann WK, Wilson SJ, Tlsty TD, Lees E, Harper JW, Elledge SJ, Reed SI. 1994. P53-dependent inhibition of cyclin-dependent kinase activities in human fibroblasts during radiation-induced G1 arrest. *Cell* 76:1013–1023.

Ferguson RL, Maller JL. 2010. Centrosomal localization of cyclin E-Cdk2 is required for initiation of DNA synthesis. *Curr Biol* 20:856–860.

Giri S, Aggarwal V, Pontis J, Shen Z, Chakraborty A, Khan A, Mizzen C, Prasanth KV, Ait-Si-Ali S, Ha T, Prasanth SG. 2015. The preRC protein ORCA organizes heterochromatin by assembling histone H3 lysine 9 methyltransferases on chromatin. *Elife* 4: e06496.

Gruber R, Zhou Z, Sukchev M, Joerss T, Frappart PO, Wang ZQ. 2011. MCPH1 regulates the neuroprogenitor division mode by coupling the centrosomal cycle with mitotic entry through the Chk1-Cdc25 pathway. *Nat Cell Biol* 13:1325–1334.

Hinchcliffe EH, Sluder G. 2001. It takes two to tango: Understanding how centrosome duplication is regulated throughout the cell cycle. *Genes Dev* 15:1167–1181.

Hoyer-Hansen M, Jaattela M. 2008. Autophagy: An emerging target for cancer therapy. *Autophagy* 4:574–580.

Jackson SJ, Singletary KW, Venema RC. 2007. Sulforaphane suppresses angiogenesis and disrupts endothelial mitotic progression and microtubule polymerization. *Vascul Pharmacol* 46:77–84.

Jung CH, Jun CB, Ro SH, Kim YM, Otto NM, Cao J, Kundu M, Kim DH. 2009. ULK-Atg13-FIP200 complexes mediate mTOR signaling to the autophagy machinery. *Mol Biol Cell* 20:1992–2003.

Kabeya Y, Mizushima N, Ueno T, Yamamoto A, Kirisako T, Noda T, Kominami E, Ohsumi Y, Yoshimori T. 2000. LC3, a mammalian homologue of yeast Apg8p, is localized in autophagosome membranes after processing. *EMBO J* 19:5720–5728.

Lai PY, Wang CY, Chen WY, Kao YH, Tsai HM, Tachibana T, Chang WC, Chung BC. 2011. Steroidogenic Factor 1 (NR5A1) resides in centrosomes and maintains genomic stability by controlling centrosome homeostasis. *Cell Death Differ* 18:1836–1844.

Lambrus BG, Daggubati V, Uetake Y, Scott PM, Clutario KM, Sluder G, Holland AJ. 2016. A USP28-53BP1-p53-p21 signaling axis arrests growth after centrosome loss or prolonged mitosis. *J Cell Biol* 214:143–153.

Lin YH, Lin YM, Teng YN, Hsieh TY, Lin YS, Kuo PL. 2006. Identification of ten novel genes involved in human spermatogenesis by microarray analysis of testicular tissue. *Fertil Steril* 86:1650–1658.

Meitinger F, Anzola JV, Kaulich M, Richardson A, Stender JD, Benner C, Glass CK, Dowdy SF, Desai A, Shiau AK, Oegema K. 2016. 53BP1 and USP28 mediate p53 activation and G1 arrest after centrosome loss or extended mitotic duration. *J Cell Biol* 214:155–166.

Mikule K, Delaval B, Kaldis P, Jurczyk A, Hergert P, Doxsey S. 2007. Loss of centrosome integrity induces p38-p53-p21-dependent G1-S arrest. *Nat Cell Biol* 9:160–170.

Mizushima N, Noda T, Yoshimori T, Tanaka Y, Ishii T, George MD, Klionsky DJ, Ohsumi M, Ohsumi Y. 1998. A protein conjugation system essential for autophagy. *Nature* 395:395–398.

Morgan DO. 1995. Principles of CDK regulation. *Nature* 374:131–134.

Pagano M, Draetta G, Jansen-Durr P. 1992. Association of cdk2 kinase with the transcription factor E2F during S phase. *Science* 255:1144–1147.

Rosler OG, Thiel G. 2017. Specificity of stress-responsive transcription factors Nrf2, ATF4, and AP-1. *J Cell Biochem* 118:127–140.

Teng YN, Liao MH, Lin YB, Kuo PL, Kuo TY. 2010. Expression of *lrwd1* in mouse testis and its centrosomal localization. *Int J Androl* 33:832–840.

Tsang WY, Spektor A, Vijayakumar S, Bista BR, Li J, Sanchez I, Duensing S, Dynlacht BD. 2009. Cep76, a centrosomal protein that specifically restrains centriole reduplication. *Dev Cell* 16:649–660.

Wang CY, Huang EY, Huang SC, Chung BC. 2015. DNA-PK/Chk2 induces centrosome amplification during prolonged replication stress. *Oncogene* 34:1263–1269.

Wang CY, Kao YH, Lai PY, Chen WY, Chung BC. 2013. Steroidogenic factor 1 (NR5A1) maintains centrosome homeostasis in steroidogenic cells by restricting centrosomal DNA-dependent protein kinase activation. *Mol Cell Biol* 33:476–484.

## SUPPORTING INFORMATION

---

Additional supporting information may be found in the online version of this article at the publisher's web-site.